Electrocatalytic Reduction of Disulfide Bonds in Antibodies

Serge Ruccolo,*[1] Marion Emmert,[1] Cecilia Bottecchia,[1] Yangzhong Qin,[2] Rodell Barrientos,[2] Kelly Raymond,[2] Monica Haley[2]

[1] Process Research and Development, Merck & Co., Inc., Rahway, NJ 07065, USA

[2] Analytical Research and Development, Merck & Co., Inc., Rahway, NJ 07065, USA

ABSTRACT: In most FDA-approved antibody-drug conjugates, cysteines generated through reduction of the native interchain disulfide bonds in monoclonal antibodies (mAbs) are conjugated with maleimide-based cytotoxic payloads. Despite being key to efficiently producing well-defined conjugates, selective disulfide reduction strategies are severely underdeveloped. Herein, we report a vitamin B_{12}-catalyzed, electrochemically driven protocol that efficiently reduces disulfide bonds in various aqueous buffers and at a broad pH range. This robust and simple method is suitable for disulfide reductions of substrates ranging from biologically relevant small molecules to large proteins. Finally, one-pot reduction/conjugation of disulfide bonds in mAbs was achieved to access antibody conjugates.

Cysteine holds a special place amongst all amino acids, due to the rich chemistry of its redox active nucleophilic thiol functional group. Indeed, numerous enzymes leverage the chemistry of the thiol moiety of cysteine in their active site to activate substrates.[1] Moreover, disulfide bonds formed through the oxidation of two cysteine residues are an essential feature of proteins and play crucial roles in protein structure, stability, and function.[2] Outside of metabolic pathways, the unique chemistry of cysteines is also heavily leveraged in antibody-drug conjugates (ADCs).[3,4] Covalent attachment of maleimide-based cytotoxic payloads to cysteine residues generated from the reduction of native disulfide bonds in monoclonal antibodies (mAbs) is the preferred bioconjugation strategy for most FDA-approved ADCs (A).[5–7]

While a breadth of chemical and enzymatic methods have been developed for thiol oxidation to disulfides,[8–10] the reverse reaction of disulfide reduction to thiols has received very little attention and, to this day, is exclusively achieved using stoichiometric amounts of reducing agents.[11] For example, reducing the internal disulfide bonds in mAbs for bioconjugation in ADCs typically requires stoichiometric reagents such as tris(2-carboxyethyl)phosphine (TCEP)[12,13] or other water-soluble phosphines (Figure 1B).[14] The inherent reactivity of these reductants results in poor site-selectivity, and can affect mAbs' integrity, downstream conjugation, and purification.[15,16] Notably, there are no general methods to reduce disulfide bonds catalytically for mAbs, and only very few examples of catalytic hydrogenations of small molecule disulfides.[17] Importantly, identifying an efficient catalyst for disulfide reduction in mAbs could address several previously mentioned shortcomings by, for

example, modulating site-selectivity through catalyst design, or replacing stoichiometric reagents with alternative driving forces.

Electrochemistry has garnered a lot of interest in synthetic chemistry as a mean to provide a greener redox driving force and has even started to appear in large scale pharmaceutical manufacturing processes.[18,19] The direct electrochemical reduction of disulfides such as cystine at various electrodes has been reported before, albeit under low pH conditions incompatible with the delicate nature of most large molecules (e.g. peptides or mAbs).[20,21] Therefore, an electrocatalytic approach that combines efficient reduction of a catalyst at the electrode surface with bulk-solution reaction between the catalyst and the target disulfides under mild aqueous conditions is more likely to succeed.[22] Fortunately, singular spectroscopic and electrochemical studies have shown that metalloporphyrinoids have promising reactivity towards disulfides (Figure 1C), but have yet to be translated into a synthetic method.[23–26] Herein, we report a catalytic system for the reduction of disulfide bonds leveraging the catalytic activity of metalloporphyrinoids and using electrochemistry as the driving force (Figure 1D). This system is successful under mild aqueous conditions compatible with a wide range of substrates, including small molecules, proteins, and mAbs. We further demonstrate the use of this method to produce antibody conjugates in a one-pot reduction/conjugation approach.

We first sought to confirm the electrocatalytic activity of metalloporphyrins using cyclic voltammetry (CV) and a small molecule model substrate, namely *N,N'*-dicarbobenzoxy-L-cystine (**1**). The direct reduction of **1** in 100 mM potassium phosphate buffer at pH 7 happens on a glassy
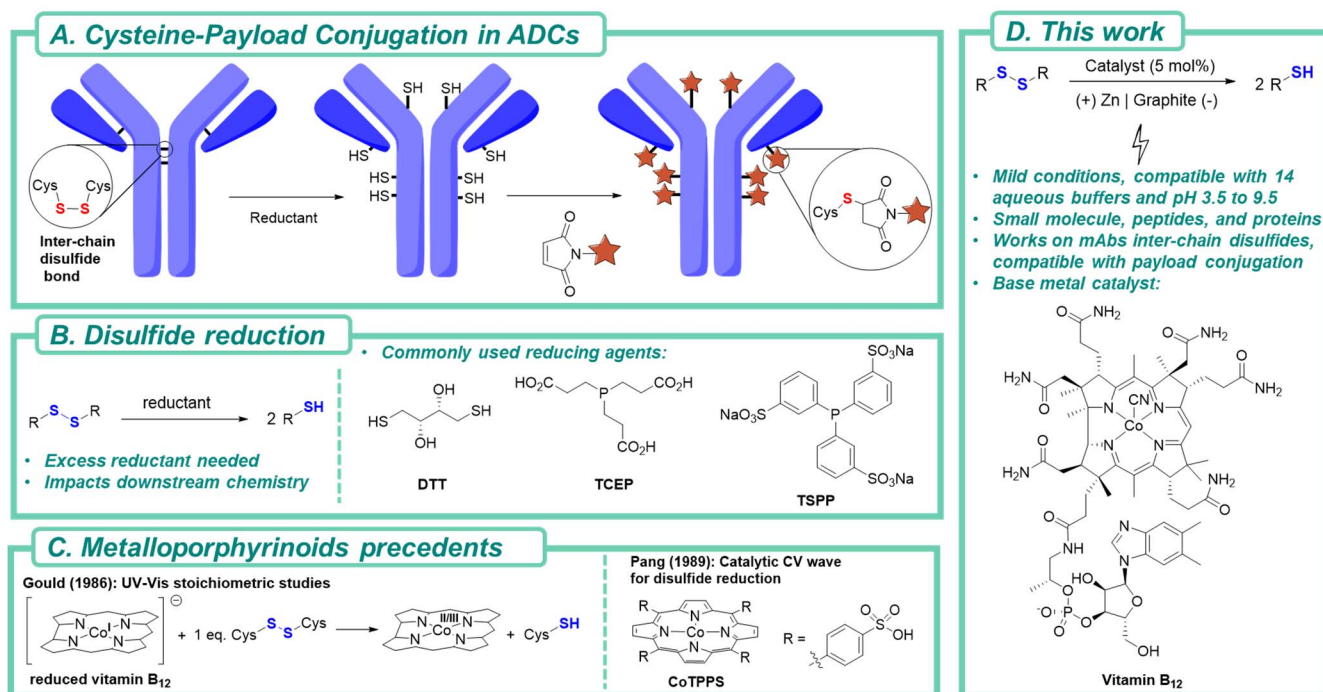
Figure 1: A) Typical ADC synthesis via a 2-step reduction and bioconjugation. B) Previous state of the art for disulfide reduction. C) Precents for metalloporphyrin reactivity towards disulfides. D) Summary of this work findings.

carbon working electrode below -1.6 V (vs Ag/AgCl). We then explored the CV of several metal porphyrinoids (See SI for details and structures) to search for catalytic waves in the presence of **1** indicative of catalytic activity.[27,28] Notably, vitamin B_{12} (VB$_{12}$), 5,10,15,20-tetrakis(4-sulfonatophenyl)porphyrinato iron(III) chloride (FeTPPS), and hemin all exhibited large catalytic currents at the different M(II) to M(I) reduction potentials (-0.89, -0.84, and ~-1.2 V vs Ag/AgCl for VB$_{12}$, FeTTPS, and hemin, respectively; Figure 2A)[24,29,30] confirming their catalytic activity for disulfide reduction of **1**. Kinetic treatment of the resulting S-curves afforded large rate constants of 2.8×10^7 M.s^{-1}, 1.5×10^6 M.s^{-1} and 6.4×10^6 M.s^{-1} for the presumed 2-electron reduction of **1** catalyzed by VB$_{12}$, FeTPPS, and hemin, respectively.[31,32]

To further elucidate the mechanism for electrocatalytic disulfide reduction, we focused on VB$_{12}$ since several potential catalytic intermediates have been reported.[33,34] We observed that the reaction between the electrochemically generated reduced Co(I) species and excess **1** yields the previously characterized Co(III)-cysteine adduct by UV-Vis spectroscopy (Figure 2B).[35] Based on the established VB$_{12}$ reactivity,[36-38] the Co(I) most likely reacts via nucleophilic attack on the disulfide, pushing the two electrons of the disulfide bond to the leaving thiolate. Additionally, the catalytic wave in the CV shows very little correlation with pH (see SI), suggesting that proton transfer to either the disulfide or the reduced thiol is not rate determining. Therefore, we propose the following mechanism for the catalytic reduction of disulfide by VB$_{12}$: (1) stepwise electrochemical reduction of Co(III) to Co(II), then to Co(I) accompanied by removal of the cyano ligand, (2) nucleophilic attack from the Co(I) to the disulfide to form a Co(III)-thiolate adduct and expulsion of a thiolate, (3) reduction
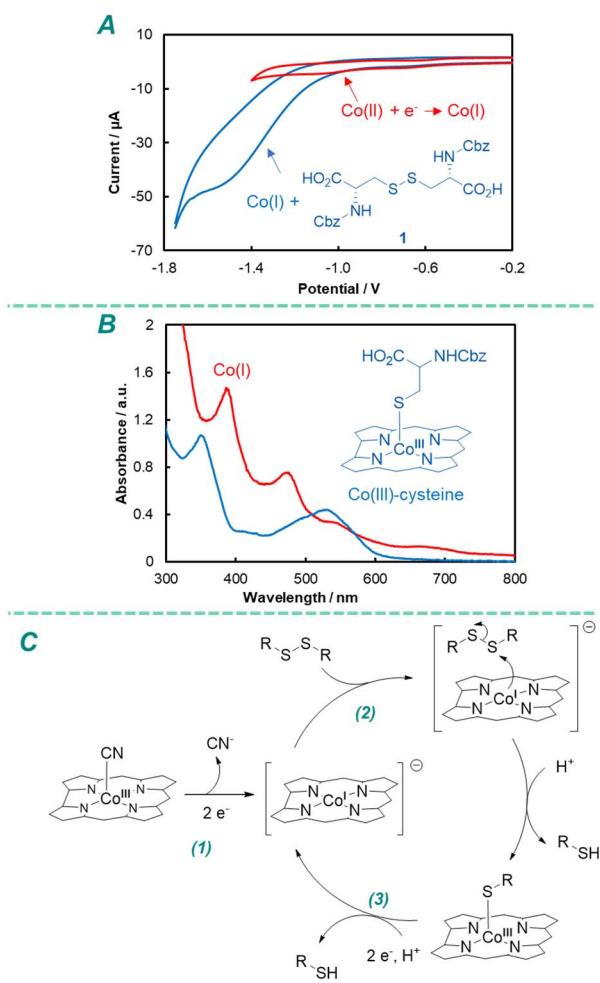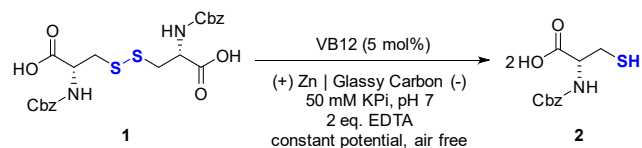

Figure 2: A) Cyclic voltammetry of VB12 without (—) and with **1** (—). B) UV-Vis spectrum of Co(I) before (—) and after adding **1** (—). C) proposed catalytic cycle for VB$_{12}$.

of the Co(III)-thiolate down to Co(I) accompanied expulsion and protonation of the thiolate (Figure 2C).

With promising results from the CV and mechanistic insights, we then sought to conduct a synthetic scale bulk electrolysis reduction of **1** in the presence of metalloporphyrinoids exhibiting electrocatalytic activity. We were pleased to observe complete reduction to N-carbobenzoxy-L-cysteine **2** with 5 mol% of either VB$_{12}$ or FeTPPS (constant potential: -0.6 V cell potential for VB$_{12}$; -0.3 V for FeTPPS; see Table 1, entries 1 and 3) under a blanket of nitrogen, in an undivided cell (glassy carbon cathode, zinc anode, 50 mM potassium phosphate buffer, 2 equiv EDTA). In contrast, hemin showed lower performance, due to competition with hydrogen evolution (entry 4). We decided to focus on VB$_{12}$, because of its commercial availability as a common food additive. Excitingly, the catalyst loading for VB$_{12}$ can be further lowered to 0.05 mol% and shows no decrease in conversion upon an extended reaction time of 18h (entry 2). The constitution of the anode was found to be critical. While Mg and Ni anodes show satisfactory conversion of 95% and 85% (entries 5 and 6), other materials such as stainless steel (34%), Al (2%) and Cu (8%) led to poor performance (entries 7, 8, and 9). Zn was ultimately chosen as the best anode because of its ability to maintain a constant cell potential (see the SI for details). Other carbon-based cathodes such as graphite also show excellent conversion (99%), even at lower cell potentials of -0.2 V (entry 10). EDTA was found to be crucial for this reaction to prevent the buildup of metal salts at the anode or electroplating of the resulting metal salts at the glassy carbon cathode, which were then undergoing either direct reduction of the cystine or hydrogen evolution (entry 11). Interestingly, there is a slow background reduction of VB$_{12}$ at the Zn electrode in the absence of current (entry 12), suggesting that Zn metal or other chemical reductants could potentially be used to drive the VB$_{12}$-catalyzed reduction. This background reaction also explains the high faradaic efficiently of 110% observed. We chose to operate at constant potential to avoid drifting towards potentials at which hydrogen evolution or direct disulfide reduction at the cathode would occur. At much lower potentials (<-1V cell potential), efficient reduction of **1** was indeed observed in the absence of catalyst. As expected from the well-known O$_2$ sensitivity of Co(I),[26] an inert atmosphere is crucial and the presence of air completely shuts down catalysis (entry 14). We demonstrated compatibility with fourteen different buffers containing carboxylates (acetate, citrate, malate, succinate), sulfonates (MES, HEPES, MOPS), imidazoles, alcohols, and amines (BIS-TRIS, BIS-TRIS propane, TRIS, bicine, tricine, glycine) functionalities. Moreover, several organic co-solvents are tolerated, e.g., acetonitrile, acetone, dimethyl sulfoxide, dimethylacetamide (up to 6 vol%), ethanol and isopropanol (tolerated up to 25 vol%) (see SI for details).

With optimized conditions in hand, we sought to interrogate the substrate scope for this reaction. All reactions were performed in an N$_2$-filled undivided cell consisting of a graphite cathode and zinc anode in 100 mM potassium phosphate buffer and in the presence of 10 mM of EDTA

Table 1: Results for the optimization of electrocatalytic disulfide bonds reduction of substrate 1 with metalloporphyrin catalysts.

Entry	Conditions	Conversion (%)
1	**Standard[a]**	99
2	**0.05 mol% loading [b]**	99
3	**FeTPPS as catalyst [c]**	95
4	**Hemin as catalyst**	56
5	**Mg anode**	99
6	**Ni anode**	85
7	**Stainless steel anode**	34
8	**Al anode**	2
9	**Cu anode**	8
10	**Graphite cathode [d]**	99
11	**No EDTA**	56
12	**No current [b]**	22
13	**No VB$_{12}$**	1
14	**In air**	1

[a] Reaction time is approximately 3 h or when the current fell below -0.1 mA. -0.6 V cell potential. [b] reaction time: 18h. [c] -0.3 V cell potential. [d] -0.2 V cell potential.

under constant potential at -0.2 V and catalytic VB$_{12}$ (see SI for details). We first focused on reducing disulfides in an array of small molecules such as *trans*-4,5-Dihydroxy-1,2-dithiane (oxidized dithiothreitol (DTT)) and 2,2'-dipyridyldisulfide. Both are reduced in high yields (88% and 99% disulfide conversion, respectively; Figure 3A). Biologically relevant molecules such as dihydrolipoic acid, glutathione and coenzyme A can be obtained from the corresponding disulfides with efficient conversions of 94%, 97% and 91%.

In a next step, we decided to test the compatibility of our new method with a set of biomolecules. Excitingly, we were able to successfully reduce internal disulfide bonds in medium-sized peptides such as the therapeutic hormone oxytocin (1.01 kDa) and the hormone somatostatin (1.64 kDa) with 95% and 98% conversion respectively (Figure 3B). Furthermore, the 3 disulfide bonds in insulin (5.78 kDa) can also successfully be reduced (99% conversion). This reaction generates the disconnected A and B peptide chains, whose presence was confirmed by mass spectrometry and quantified by reversed phase liquid chromatography (RPLC). Notably, VB$_{12}$ is also capable of reducing disulfide bonds of larger proteins such as lysozyme, a 14.3 kDa protein containing 4 disulfide bonds[39] (77% conversion). Larger protein assemblies such as fibrinogen, a 340 kDa
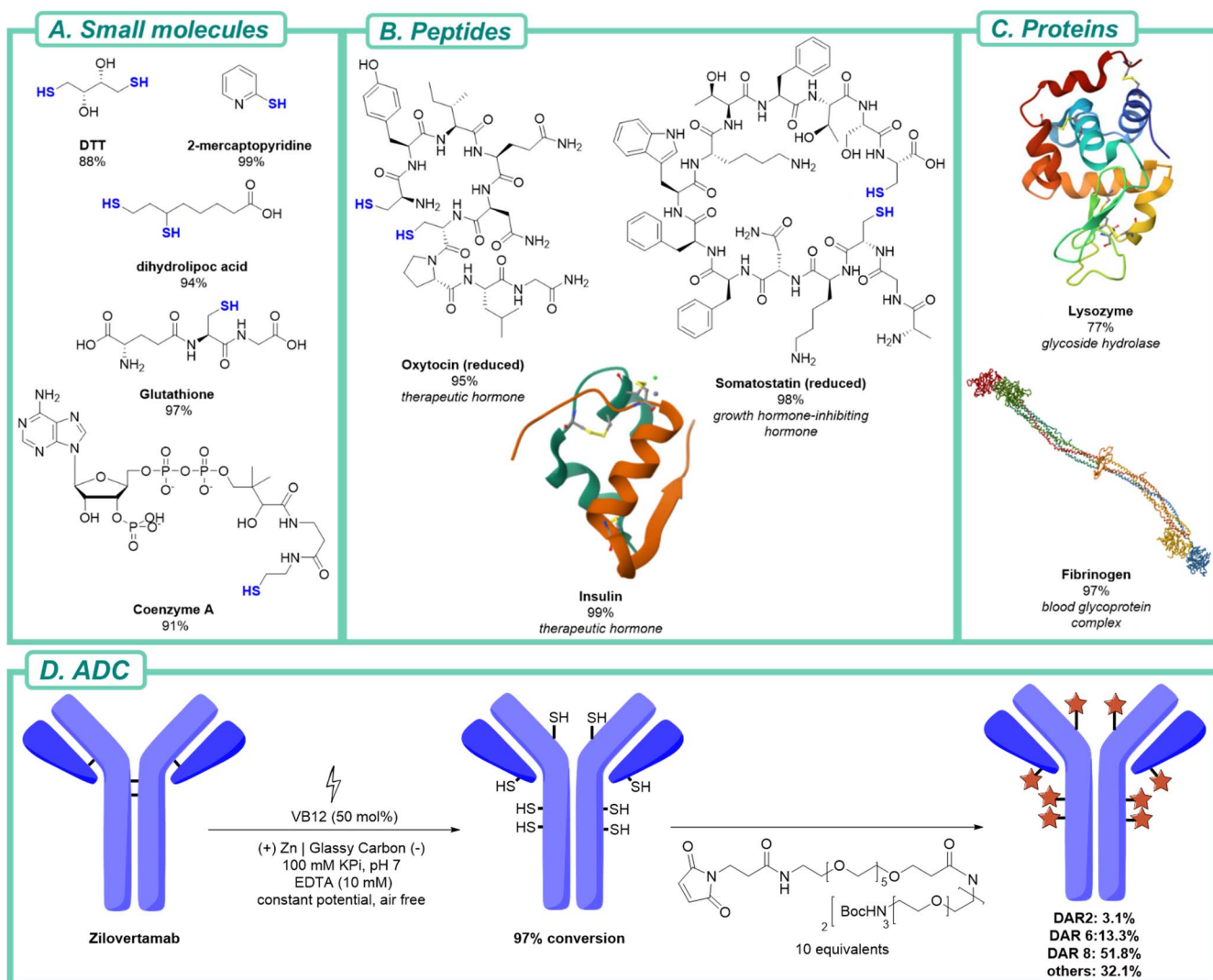
Figure 3: Substrate scope for the VB_{12} catalyzed disulfide reduction, the percentage represent disulfide conversion by chromatography. See SI for details on individual reactions.

dimer containing 29 disulfide bonds between 2 pairs of 3 non-identical chains[40] can also be reduced efficiently with 97% yield (Figure 3C). The formation of reduced chains was confirmed by mass spectrometry and RPLC. Importantly, high concentrations (3 M) of denaturing agents such as guanidinium hydrochloride are tolerated well; this additive is required for reactions with insulin and fibrinogen to avoid aggregation and precipitation of the reduced proteins chains.

To test if the established disulfide reduction protocol would be a suitable alternative to traditional stoichiometric reductants for ADC synthesis, we shifted our focus to Zilovertamab, an IgG1 antibody (148 kDa) which targets the tyrosine kinase-like orphan receptor 1 (ROR1). Zilovertamab is currently under investigation as part of an ADC with vedotin for the treatment of lymphoid cancers.[41,42] When exposed to a slightly modified reaction protocol (See SI), electrocatalytic reduction of Zilovertamab is observed. Particularly, reductive cleavage of the internal disulfide bonds lead to the detection of the mAb light and heavy chains by mass spectrometry, RPLC, and capillary electrophoresis (97% conversion). Electrochemical reduction

followed by bioconjugation with a maleimide N-(Mal-PEG6)-N-bis(PEG3-Boc) in one pot showed the formation of several new species corresponding to cysteine-maleimide adducts by hydrophobic interaction chromatography (HIC).[43] The ratio of antibody to maleimide, referred to as drug to antibody ratio (DAR), is a key attribute of ADCs typically correlated with potency.[4] Mass spectrometry confirmed the formation of the DAR 8 species as the major species, which confirms that VB_{12} can reduce all 4 interchain disulfide bonds in IgG1 mAbs successfully, while not interfering with bioconjugation after electrolysis (Figure 3D). Notably, no DAR 0 is observed, confirming the high activity of VB_{12}. For reference, the distribution from traditional TCEP reduction protocols yields a relatively comparable distribution of DAR 2: 13.3%, DAR 6: 15.7%, DAR 8: 66.3%, others: 4.7%.

In conclusion, we are disclosing a new method for the electrochemically driven reduction of disulfide bonds catalyzed by metalloporphyrins. The method is simple, robust across a wide pH window, and compatible with many buffers systems. The method can be applied to various disulfide-containing small molecules as well as larger peptides,

proteins and, importantly, mAbs. The method can be used to produce antibody conjugates under mild, biocompatible conditions. We believe this method has potential for future improvements, especially in the context of ADCs production. Further catalyst design could enable higher efficiency and selectivity, while electrochemistry could replace stoichiometric reducing agents with more benign sacrificial metal anodes. We therefore believe this method is likely to have many exciting applications given the ever-increasing number of ADCs making their way to clinical trials and FDA approval.

ASSOCIATED CONTENT

This material is available free of charge via the Internet at http://pubs.acs.org.

AUTHOR INFORMATION

Corresponding Author

* Serge Ruccolo – Process Research and Development, Merck & Co., Inc., Rahway, New Jersey 07065, United States; email: serge.ruccolo@merck.com

ACKNOWLEDGMENT

REFERENCES

(1) Giles, N. M.; Giles, G. I.; Jacob, C. Multiple Roles of Cysteine in Biocatalysis. *Biochem. Biophys. Res. Commun.* **2003**, *300* (1), 1–4. https://doi.org/10.1016/S0006-291X(02)02770-5.

(2) Fass, D.; Thorpe, C. Chemistry and Enzymology of Disulfide Cross-Linking in Proteins. *Chem. Rev.* **2018**, *118* (3), 1169–1198. https://doi.org/10.1021/acs.chemrev.7b00123.

(3) Fu, Z.; Li, S.; Han, S.; Shi, C.; Zhang, Y. Antibody Drug Conjugate: The "Biological Missile" for Targeted Cancer Therapy. *Signal Transduct. Target. Ther.* **2022**, *7* (1). https://doi.org/10.1038/s41392-022-00947-7.

(4) Sasso, J. M.; Tenchov, R.; Bird, R.; Iyer, K. A.; Ralhan, K.; Rodriguez, Y.; Zhou, Q. A. The Evolving Landscape of Antibody-Drug Conjugates: In Depth Analysis of Recent Research Progress. *Bioconjug. Chem.* **2023**. https://doi.org/10.1021/acs.bioconjchem.3c00374.

(5) Cal, P. M. S. D.; Bernardes, G. J. L.; Gois, P. M. P. Cysteine-Selective Reactions for Antibody Conjugation. *Angew. Chemie - Int. Ed.* **2014**, *53* (40), 10585–10587. https://doi.org/10.1002/anie.201405702.

(6) Walsh, S. J.; Bargh, J. D.; Dannheim, F. M.; Hanby, A. R.; Seki, H.; Counsell, A. J.; Ou, X.; Fowler, E.; Ashman, N.; Takada, Y.; Isidro-Llobet, A.; Parker, J. S.; Carroll, J. S.; Spring, D. R. Site-Selective Modification Strategies in Antibody-Drug Conjugates. *Chem. Soc. Rev.* **2021**, *50* (2), 1305–1353. https://doi.org/10.1039/d0cs00310g.

(7) Spears, R. J.; McMahon, C.; Chudasama, V. Cysteine Protecting Groups: Applications in Peptide and Protein Science. *Chem. Soc. Rev.* **2021**, *50* (19), 11098–11155. https://doi.org/10.1039/d1cs00271f.

(8) Spear, A.; Orativskyi, O.; Tran, S.; Zubieta, J. A.; Doyle, R. P. Rapid, Green Disulphide Bond Formation in Water Using the Corrin Dicyanocobinamide. *Chem. Commun.* **2023**. https://doi.org/10.1039/d3cc02646a.

(9) He, R.; Pan, J.; Mayer, J. P.; Liu, F. The Chemical Methods of Disulfide Bond Formation and Their Applications to Drug Conjugates. *Curr. Org. Chem.* **2019**, *23* (25), 2802–2821. https://doi.org/10.2174/1385272823666191202111723.

(10) Zhang, N.; Müller, B.; Kirkeby, T. Ø.; Kara, S.; Loderer, C. Development of a Thioredoxin-Based Cofactor Regeneration System for NADPH-Dependent Oxidoreductases. *ChemCatChem* **2022**, *14* (7). https://doi.org/10.1002/cctc.202101625.

(11) Mthembu, S. N.; Sharma, A.; Albericio, F.; de la Torre, B. G. Breaking a Couple: Disulfide Reducing Agents. *ChemBioChem* **2020**, *21* (14), 1947–1954. https://doi.org/10.1002/cbic.202000092.

(12) Jackson, D. Y. Processes for Constructing Homogeneous Antibody Drug Conjugates. *Org. Process Res. Dev.* **2016**, *20* (5), 852–866. https://doi.org/10.1021/acs.oprd.6b00067.

(13) Kang, M. S.; Kong, T. W. S.; Khoo, J. Y. X.; Loh, T. P. Recent Developments in Chemical Conjugation Strategies Targeting Native Amino Acids in Proteins and Their Applications in Antibody-Drug Conjugates. *Chem. Sci.* **2021**, *12* (41), 13613–13647. https://doi.org/10.1039/d1sc02973h.

(14) Procopio-Melino, R.; Kotch, F. W.; Prashad, A. S.; Gomes, J. M.; Wang, W.; Arve, B.; Dawdy, A.; Chen, L.; Sperry, J.; Hosselet, C.; He, T.; Kriz, R.; Lin, L.; Marquette, K.; Tchistiakova, L.; Somers, W.; Rouse, J. C.; Zhong, X. Cysteine Metabolic Engineering and Selective Disulfide Reduction Produce Superior Antibody-Drug-Conjugates. *Sci. Rep.* **2022**, *12* (1), 1–11. https://doi.org/10.1038/s41598-022-11344-z.

(15) Kantner, T.; Watts, A. G. Characterization of Reactions between Water-Soluble Trialkylphosphines and Thiol Alkylating Reagents: Implications for Protein-Conjugation Reactions. *Bioconjug. Chem.* **2016**, *27* (10), 2400–2406. https://doi.org/10.1021/acs.bioconjchem.6b00375.

(16) Jackson, D. Y. Processes for Constructing Homogeneous Antibody Drug Conjugates. *Org. Process Res. Dev.* **2016**, *20* (5), 852–866. https://doi.org/10.1021/acs.oprd.6b00067.

(17) Novakova, E. K.; McLaughlin, L.; Burch, R.; Crawford, P.; Griffin, K.; Hardacre, C.; Hu, P.; Rooney, D. W. Palladium-Catalyzed Liquid-Phase Hydrogenation/Hydrogenolysis of Disulfides. *J. Catal.* **2007**, *249* (1), 93–101. https://doi.org/10.1016/j.jcat.2007.04.002.

(18) Tay, N. E. S.; Lehnherr, D.; Rovis, T. Photons or Electrons? A Critical Comparison of Electrochemistry and Photoredox Catalysis for Organic Synthesis. *Chem. Rev.* **2022**, *122* (2), 2487–2649. https://doi.org/10.1021/acs.chemrev.1c00384.

(19) Lehnherr, D.; Chen, L. Overview of Recent Scale-Ups in Organic Electrosynthesis (2000 – 2023). **2023**. https://doi.org/10.1021/acs.oprd.3c00340.

(20) Seidler, J.; Bernhard, R.; Haufe, S.; Neff, C.; Gärtner, T.; Waldvogel, S. R. From Screening to Scale-Up: The DoE-Based Optimization of Electrochemical Reduction of l-Cystine at Metal Cathodes. *Org. Process Res. Dev.* **2021**, *25* (12), 2622–2630. https://doi.org/10.1021/acs.oprd.1c00153.

(21) Ralph, T. R.; Hitchman, M. L.; Millington, J. P.; Walsh, F. C. The Importance of Batch Electrolysis Conditions during the Reduction of L-Cystine Hydrochloride. *J. Electrochem. Soc.* **2005**, *152* (3), D54. https://doi.org/10.1149/1.1858831.

(22) Savéant, J.; Costentin, C. Enzymatic Catalysis of Electrochemical Reactions. In *Elements of Molecular and Biomolecular Electrochemistry*; 2019; pp 383–437. https://doi.org/10.1002/9781119292364.ch6.

(23) Wang, Z.; Pang, D. Electrocatalysis of Metalloporphyrins. Part 9. Catalytic Electroreduction of Cystine Using Water-Soluble Cobalt Porphyrins. *J. Electroanal. Chem.* **1990**, *283* (1–2), 349–358. https://doi.org/10.1016/0022-0728(90)87400-E.

(24) Chen, S. M. The Electrocatalytic Reactions of Cysteine and Cystine by Water-Soluble Iron Porphyrin, Manganese Porphyrin and Iron(II) Phenanthrolines. *Electrochim. Acta* **1997**, *42* (11), 1663–1673. https://doi.org/10.1016/S0013-4686(96)00307-6.

(25) Li, Z.; Shanmuganathan, A.; Ruetz, M.; Yamada, K.; Lesniak,

N. A.; Kra, B.; Brunold, T. C.; Koutmos, M.; Banerjee, R. Coordination Chemistry Controls the Thiol Oxidase Activity of the B 12 -Trafficking Protein CblC. **2017**, *292* (Ii), 9733–9744. https://doi.org/10.1074/jbc.M117.788554.

(26) Pillai, G. C.; Gould, E. S. Electron Transfer. 79. Reductions of Organic Disulfides by Vitamin B12s (Cob(I)Alamin). *Inorg. Chem.* **1986**, *25* (19), 3353–3356. https://doi.org/10.1021/ic00239a008.

(27) Costentin, C.; Savéant, J. M. Homogeneous Molecular Catalysis of Electrochemical Reactions: Manipulating Intrinsic and Operational Factors for Catalyst Improvement. *J. Am. Chem. Soc.* **2018**, *140* (48), 16669–16675. https://doi.org/10.1021/jacs.8b09154.

(28) Ruccolo, S.; Brito, G.; Christensen, M.; Itoh, T.; Mattern, K.; Stone, K.; Strotman, N. A.; Sun, A. C. Electrochemical Recycling of Adenosine Triphosphate in Biocatalytic Reaction Cascades. *J. Am. Chem. Soc.* 2022, *144* (49), 22582–22588. https://doi.org/10.1021/jacs.2c08955.

(29) Leva, D.; Saveant, J. M. Electrochemistry of Vitamin B12. I. Role of the Base-On/Base-Off Reaction in the Oxidoreduction Mechanism of the B12r-B12s System. *J. Am. Chem. Soc.* **1976**, *98* (9), 2652–2658. https://doi.org/10.1021/ja00425a039.

(30) Dereven'kov, I. A.; Salnikov, D. S.; Silaghi-Dumitrescu, R.; Makarov, S. V.; Koifman, O. I. Redox Chemistry of Cobalamin and Its Derivatives. *Coord. Chem. Rev.* **2016**, *309*, 68–83. https://doi.org/10.1016/j.ccr.2015.11.001.

(31) Rountree, E. S.; McCarthy, B. D.; Eisenhart, T. T.; Dempsey, J. L. Evaluation of Homogeneous Electrocatalysts by Cyclic Voltammetry. *Inorg. Chem.* **2014**, *53* (19), 9983–10002. https://doi.org/10.1021/ic500658x.

(32) Cyrille, C.; Jean-Michel, S. Multielectron, Multistep Molecular Catalysis of Electrochemical Reactions: Benchmarking of Homogeneous Catalysts. *ChemElectroChem* **2014**, *1* (7), 1226–1236. https://doi.org/10.1002/celc.201300263.

(33) Sajan, A.; Birke, R. L. The Reductive Cleavage Mechanism and Complex Stability of Glutathionyl-Cobalamin in Acidic Media. *Electroanalysis* **2016**, *28* (11), 2743–2753. https://doi.org/10.1002/elan.201600341.

(34) Mascarenhas, R.; Guha, A.; Li, Z.; Ruetz, M.; An, S.; Seravalli, J.; Banerjee, R. Cobalt – Sulfur Coordination Chemistry Drives B 12 Loading onto Methionine Synthase. **2023**. https://doi.org/10.1021/jacs.3c07941.

(35) Suarez-Moreira, E.; Hannibal, L.; Smith, C. A.; Chavez, R. A.; Jacobsen, D. W.; Brasch, N. E. A Simple, Convenient Method to Synthesize Cobalamins: Synthesis of Homocysteinylcobalamin, N-Acetylcysteinylcobalamin, 2-N-Acetylamino-2- Carbomethoxyethanethiolatocobalamin, Sulfitocobalamin and Nitrocobalamin. *Dalt. Trans.* **2006**, No. 44, 5269–5277. https://doi.org/10.1039/b610158e.

(36) Costentin, C.; Robert, M.; Save, J. Does Catalysis of Reductive Dechlorination of Tetra- and Trichloroethylenes by Vitamin B12 and Corrinoid-Based Dehalogenases Follow an Electron Transfer Mechanism? **2005**, 12154–12155.

(37) Zhu, Q.; Costentin, C.; Stubbe, J.; Nocera, D. G. Chemical Science Biology and Photoredox Chemistry †. **2023**, 6876–6881. https://doi.org/10.1039/d3sc01867a1.

(38) Wdowik, T.; Gryko, D. C – C Bond Forming Reactions Enabled by Vitamin B 12 Opportunities and Challenges. **2022**. https://doi.org/10.1021/acscatal.2c01596.

(39) Blake, C.; Koenig, D.; Mair, G.; North, A.; Phillips, D.; Sarma, V. The Three-Dimensional Structure of Hen Eggwhite Lysozyme. *Nature* **1965**, *206* (49), 757–761.

(40) Blomback, B.; Blomback, M. ENZYME THE MOLECULAR STRUCTURE OF FIBRINOGEN Annals New York Academy of Sciences. 77–97.

(41) Wang, M. L.; Barrientos, J. C.; Furman, R. R.; Mei, M.; Barr, P. M.; Choi, M. Y.; de Vos, S.; Kallam, A.; Patel, K.; Kipps, T. J.; Rule, S.; Flanders, K.; Jessen, K. A.; Ren, H.; Riebling, P. C.; Graham, P.; King, L.; Thurston, A. W.; Sun, M.; Schmidt, E. M.; Lannutti, B. J.; Johnson, D. M.; Miller, L. L.; Spurgeon, S. E. Zilovertamab Vedotin Targeting of ROR1 as Therapy for Lymphoid Cancers. *NEJM Evid.* **2022**, *1* (1), 1–11. https://doi.org/10.1056/evidoa2100001.

(42) Spurgeon, S. E.; Mei, M.; Barr, P. M.; Barrientos, J. C.; de Vos, S.; Furman, R. R.; Patel, K.; Thompson, P. A.; Choi, M. Y.; Kallam, A.; Wang, S.; Ogbu, U. C.; Nahar, A.; Wang, M. L. Waveline-001: Updated Results from a Phase 1 Dose Escalation and Cohort Expansion Study of Zilovertamab Vedotin (MK-2140) in Non-Hodgkin Lymphoma. *Blood* **2022**, *140* (Supplement 1), 6640–6641. https://doi.org/10.1182/blood-2022-163509.

(43) Bottecchia, C.; Emmert, M. H.; Barrientos, R.; Feng, Y.; Holland-Moritz, D.; Hughes, G.; Lam, Y.-H.; Regalado, E.; Ruccolo, S.; Sun, S.; Chmielowski, R.; Yang, C.; Lévesque, F. "Build Your Own" ADC Mimics: Identification of Non-Toxic Linker/Payload Mimics for HIC-Based DAR Determination, High-Throughput Optimization, and Continuous Flow Conjugation. *ChemRxiv* **2024**. https://doi.org/10.26434/chemrxiv-2024-r4m2x.

SYNOPSIS TOC (Word Style "SN_Synopsis_TOC"). If you are submitting your paper to a journal that requires a synopsis graphic and/or synopsis paragraph, see the Instructions for Authors on the journal's homepage for a description of what needs to be provided and for the size requirements of the artwork.

To format double-column figures, schemes, charts, and tables, use the following instructions:

Place the insertion point where you want to change the number of columns
From the **Insert** menu, choose **Break**
Under **Sections**, choose **Continuous**
Make sure the insertion point is in the new section. From the **Format** menu, choose **Columns**
In the **Number of Columns** box, type **1**
Choose the **OK** button

Now your page is set up so that figures, schemes, charts, and tables can span two columns. These must appear at the top of the page. Be sure to add another section break after the table and change it back to two columns with a spacing of 0.33 in.

Table 1. Example of a Double-Column Table

Column 1	Column 2	Column 3	Column 4	Column 5	Column 6	Column 7	Column 8

Authors are required to submit a graphic entry for the Table of Contents (TOC) that, in conjunction with the manuscript title, should give the reader a representative idea of one of the following: A key structure, reaction, equation, concept, or theorem, etc., that is discussed in the manuscript. Consult the journal's Instructions for Authors for TOC graphic specifications.

Insert Table of Contents artwork here